Original article

Textile Research Journal

Textile Research Journal
84(1) 3–15

DOI: 10.1177/0040517513487789
trj.sagepub.com

SAGE

Electromechanical properties of knitted wearable sensors: part I – theory

Jinfeng Wang[1,2], Hairu Long[1], Saeid Soltanian[3], Peyman Servati[3] and Frank Ko[2]

Abstract

This paper reports the development of a hexagon resistance model, based on the loop structure of a plain weft knitted fabric. This model is capable of describing the electromechanical properties of conductive knitted elastic fabrics. Based on the relationship between the resistance and the load on the fabric under biaxial extension, the equivalent resistance of the fabric was obtained by solving the circuit network equations. It was found that the circuit network is a multiple circuit parallel to the wale direction whereas it is in series along the course direction. And Holm's electrical contact theory is used to calculate the relationship between the contact resistance and the contact force in an elastic fabric sensor. The contact load and deformation between two knitting loops are calculated using the classical knitted fabric mechanics model of Kawabata and Popper.

Keywords

Hexagon resistance model, structure properties, knitting, conductive yarn, human sensory and comfort issues

With the improvement of health care, people are living longer, but with multiple and more complex health conditions.[1, 2] Health monitoring equipment is necessary, while commercially available devices are expensive, large, complex and uncomfortable to wear. Users must lie on the bed, and often the sensor has to be taped on the body or clipped on fingers. We use cardiorespiratory signs, include physiological and biochemical sensing, such as for the heartbeat and respiratory cycle, as well as motion sensing to estimate a person's health condition.[3–5] There is a need for less sophisticated health monitoring systems in clinical practice, the remote health monitoring system, rehabilitation and sports activities. Also due to the advantages of having a small size, low power and low cost, accelerometers with wearable sensor have become popular tools for objectively monitoring human activities.[6, 7] Now, the application of wearable activity monitors plays a key in so-called 'health smart home' monitoring systems to establish a health monitoring system.[8] In this system, the Internet can provide a sufficient network anywhere to connect ambulatory devices together or to connect to a specialist center supporting this system.[9–18] All health signals are sent to a specialist monitoring station where vital parameters are analyzed. But the disadvantage of smart fabrics is that the manufacturing process is complicated and the production has lower accuracy and repeatability than common health conditions.

In recent years, the application of conductive knitted fabrics in wearable sensors has received great attention, due to the unique elastic properties when compared with other fabric structures such as woven and braid.[19] Other advantages of knitted sensors are their softness and how comfortable they are because of the loop structure.

In this paper, based on the loop structure of the knitted fabric, the hexagon resistance model is developed to predict electromechanical properties of

[1]College of Textiles, Donghua University, China
[2]Department of Materials Engineering, University of British Columbia, Canada
[3]Department of Electrical and Computer Engineering, University of British Columbia, Canada

Corresponding author:
Hairu Long, College of Textiles, Donghua University, 2999 North Renmin Road, Songjiang District Shanghai. 201620 China.
Email: hrlong@dhu.edu.cn

conductive knitted elastic fabrics. The sensing mechanism is based on the change of the fabric electric resistance responding to deformation caused by an applied load. The relationship between the electric resistance and the load applied to the fabric is analyzed by using a simple fabric structure to identify the key factors such as sensitivity, repeatability and linearity of the fabric gauge. By simplifying the complex analyses, the application of these models for predicting the conductive deformation behavior of knitted fabric is very practical, especially in the case where the deformation of an elastic knitted fabric is limited in not only one direction, but also in two directions. By designing a suitable fabric structure with this model and an appropriate material, the sensitivity, repeatability and linearity of the sensor are significantly improved.

The hexagonal resistance model

Description of the model

A hexagonal model[20,21] can be chosen for a knitted fabric to closely replicate its structure. Here, it is assumed the following:

1. The projected yarn lengths (on the fabric plane) are sufficient representations of the actual lengths;
2. The fabric deformation is homogeneous;
3. The yarns are straight except at the crossing areas;
4. The ratio of yarn radius to stitch length is no greater than approximately 4%. (Actually, this is a geometric requirement).

A unit cell is comprised of a needle loop *La*, two contact interlooped segments *c*, a sinker loop *La* and two leg yarn segments *Lb*. Two unit cells contact with a needle loop along the vertical direction, while two unit cells contact with a sinker loop along the horizontal direction. In this model, the elastic fabric can be personated by a hexagonal grid formed by loop yarn segments as shown in Figure 1(a).

When a voltage is applied to a conductor formed by an elastic conductive fabric, the current flowing between the electrodes will change in accordance to the applied mechanical load. Due to the high conductivity of the material used for conductive fibers in this paper, the electric fabric can be modeled by a pure resistive circuit network model as shown in Figure 1(b).

Figure 1(b) illustrates a plain weft knitted fabric hexagonal equivalent circuit. A unit cell is comprised of two contact interlooped resistances R_c and four yarn segment resistances RL. Two unit cells contact each other with a needle loop resistance along the vertical direction, while two unit cells contact with each other with a sinker loop resistance along the horizontal direction. R_c and RL represent the electrical resistance at the contact points of the overlapped yarns and the intrinsic resistance of the conductive yarns, respectively. The contact resistance R_c is assumed to be only related to the normal contact forces acting at the crossover regions without considering their contact length. Since the needle loop and the sinker loop have similar length, both resistances are approximated by *RLa*, whereas the leg yarn segments resistances are expressed by *RLb*. The elastic fabric is modeled by a complex network formed with serial-parallel resistances, representing different yarn segments and contacts. The effects of yarn segment transfer of the loop resistance and the contact resistance will be discussed in the following sections.

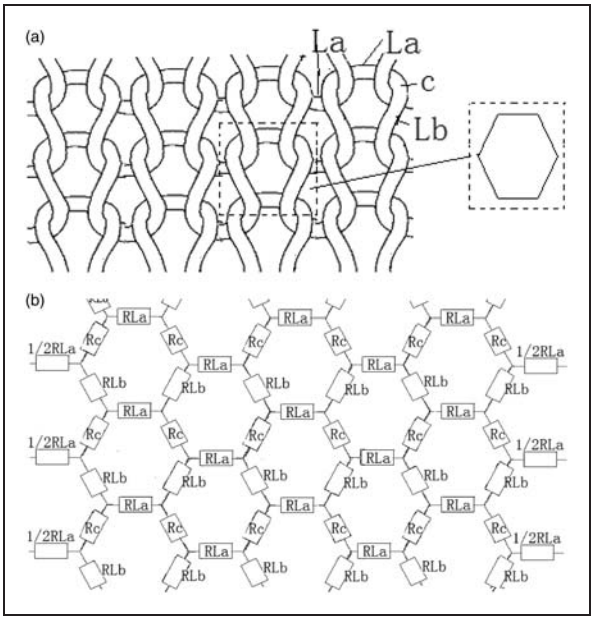

Figure 1. (a) A plain weft knitted fabric structure and (b) the hexagonal resistance model.

The equivalent resistance of the fabric is then derived from this model network according to Kirchhoff's rules. The change in resistance with the applied mechanical load can then be linked to the modification in yarn segment length and the normal force of the yarn. The latter was obtained from an empirical relationship,[22] which is the summation of the knitted loop testing experiments between the contact resistance and the normal force of yarns.

Factors affecting the resistance of elastic plain knitted fabric

When the fabric is subjected to a mechanical load, the shape of the knitted loops will change. Therefore, the contact resistance and the loop yarn segments resistance will change according to the variation of the

contact force and the yarn segment transfer in the knitted loops respectively. The following sections describe the model in detail for the yarn resistance, the yarn segment transfer of the loop resistance and the contact resistance.

Yarn segment resistance model. The yarn segment resistance R increases with tensile strain; the change can be written by differentiation in parts from the conventional resistance law as[23]

$$\frac{dR}{R} = \frac{\mathrm{d}\rho}{\rho} + \frac{dl}{l} - \frac{\mathrm{d}A}{A} \tag{1}$$

where ρ, l and A are resistivity, length and cross-sectional area of the yarn, respectively. Here, the strain in the longitudinal and radial directions for the conductive yarn with a cylindrical structure with an initial radius r can be written as

$$\varepsilon_l = \frac{dl}{l} \text{ and } \varepsilon_r = \frac{dr}{r} = -\nu\frac{dl}{l} = -\nu\varepsilon_l \tag{2}$$

respectively, using the Poisson's ratio. Using this equation, the changes in the cross-sectional area and volume of the yarn can be written as

$$\frac{\mathrm{d}A}{A} = (1+\varepsilon_r)^2 - 1 = 2\varepsilon_r + \varepsilon_r^2 = -2\nu\frac{dl}{l} + \nu^2\left(\frac{dl}{l}\right)^2 \tag{3}$$

and

$$\frac{\mathrm{d}V}{V} = \frac{dl}{l} + \frac{\mathrm{d}A}{A} = \varepsilon_l - 2\nu\varepsilon_l + \nu^2\varepsilon_l^2 = \nu^2\varepsilon_l^2 + (1-2\nu)\varepsilon_l \tag{4}$$

respectively. Assuming the resistivity $\rho = cV$ for the conductive material, where c is a constant related to the number of free electrons per atom and the atomic density, we have

$$\frac{\mathrm{d}\rho}{\rho} = c\frac{\mathrm{d}V}{V} = c\nu^2\varepsilon_l^2 + c(1-2\nu)\varepsilon_l \tag{5}$$

Using equations (1) to (5), the change in resistance can be written as

$$\frac{dR}{R} = \nu^2(c-1)\varepsilon_l^2 + [2(1-c)\nu + c + 1]\varepsilon_l \tag{6}$$

The resistance of the yarn then is

$$R = \nu^2(c-1)\varepsilon_l^2 R_0 + [2(1-c)\nu + c + 1]\varepsilon_l R_0 + R_0 \tag{7}$$

where R_0 is the resistance of the yarn under no strain. For a given material, the strain sensitivity, or gauge factor K, can be written as

$$K = \frac{dR/R}{dl/l} = \nu^2(c-1)\varepsilon_l + [2(1-c)\nu + c + 1] \tag{8}$$

For small strain values, the resistance reads

$$R = [2(1-c)\nu + c + 1]\varepsilon_l R_o + R_o \tag{9}$$

The relationship between the resistance and the strain of the silver-plating yarn is tested by a set-up including a motorized actuator (Zaber T-LSM 28) for applying the uniaxial strain and a Keithley 2400 source meter unit for supplying a voltage and reading the current synchronous with the changes in the applied strain. Figure 2(a) is the relationship between the resistance and the strain within 2%, and Figure 2(b) is the relationship between the resistance and the strain within 5%. When the silver-plating yarn is tensed within the large deformation, the change of the resistance to the strain obeys a quadratic function. When the strain is relatively low, the resistance is linear; it is like the metal wire.

In fitting the curve, $R_0 = 26.41\Omega$ and $[2(1-c)\nu + c + 1]R_o = 66.38$.

The influencing factors on the gauge factor K as expressed above are the contribution due to c and the Poisson effect, which responds to be axial stretching in an elastic material.

Figure 3 shows the silver-plating yarn before and after a tensile test. After the yarn is tensed, the change in length is given and the diameter can be measured; therefore, Poisson's ratio can be calculated

$$\nu = -\frac{\varepsilon_r}{\varepsilon_l} = -\frac{(r-r_0)/r_0}{(l-l_0)/l_0} = -\frac{(164.286-172.619)/172.619}{(59-52)/52} = 0.3586$$

Poisson's ratio of nylon is 0.28, and silver is 0.377. If 0.3586 is substitute into equation (9) and the equation in the Figure 2, it can be calculated that $c = 2.833$ and $K = 2.51$, which is in the range of the metal.

Yarn segment transfer of the loop resistance. Yarn segment transfer of the loop resistance is the fabric resistance change because of the geometry of the knitted loops. When the fabric is subjected to tension, the shape of the knitted loops will change and the length will exchange from leg yarn to needle and sinker loops, so the yarn segment resistance will exchange. Accordingly, all yarn segments resistances will change, and, after

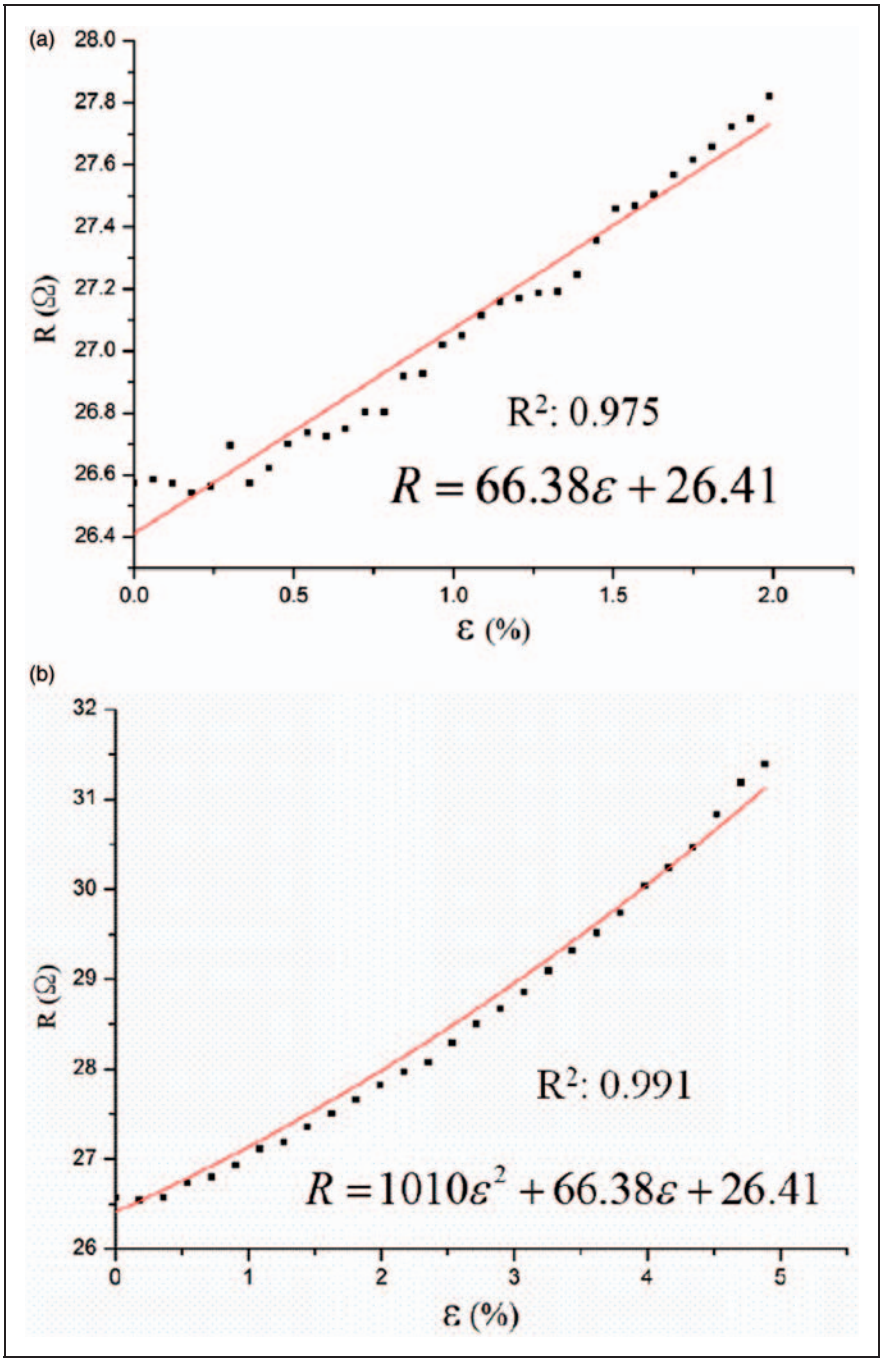

Figure 2. Resistance versus strain of the silver-plating yarn within (a) 2% and (b) 5%. The dot lines are the data obtained from the experiments and the solid lines represent the fitted curves calculated by Matlab software.

complex calculation, the fabric resistance network will change.

Relationship between the yarn segment resistance and the strain. The mechanics of a knitted fabric has been studied since the 1950s.[24–33] When a knitted fabric is subjected to a biaxial tensile load, the geometry of the knitted loops will change accordingly. The curved yarn will straighten at interlocked points. Simultaneously, the contact force at the interlooped points increases in this process.

The elastic tensile deformation of the knitted fabric leads to the following sequential steps for yarn segment transfer of the loop:

1. Straightening of the curved yarn;
2. The extension of the straightened yarn in the direction of the tensile strain;

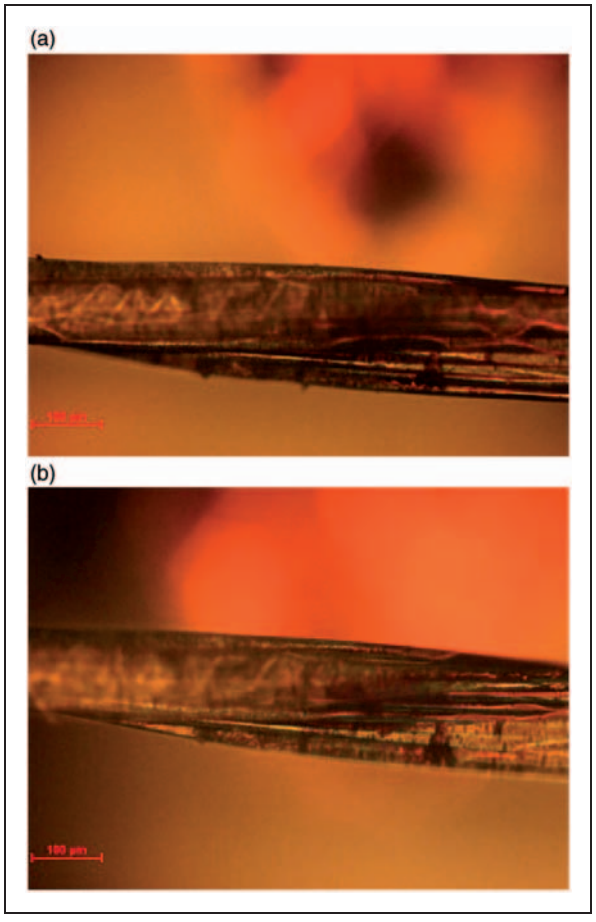

Figure 3. Silver-plating yarn (a) before and (b) after a tensile test.

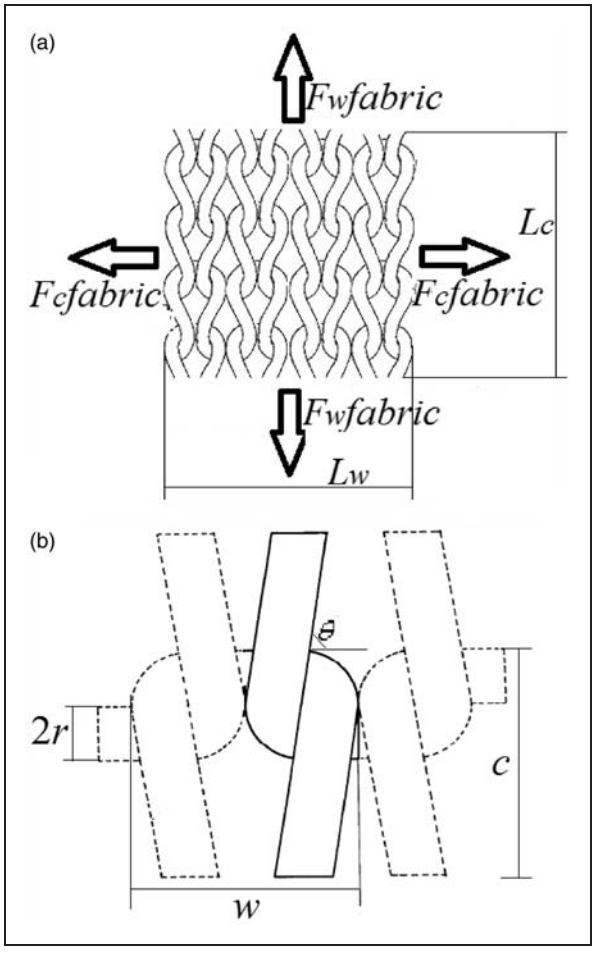

Figure 4. (a) Biaxial tension to the fabric and (b) the basic element of the structure.

3. Yarn slippage at the points where the yarn is interlaced;
4. Compressional deformation of the yarn at the points of the yarn interlaces.

While in the actual deformation process of a knitted fabric, these steps happen simultaneously. However, steps (1) and (2) are separated to simplify the analysis. The critical stretch point is when the curved yarn is straightened without elongation along the yarn axis.

When the fabric is subjected to biaxial tension, the stitch loop length of the yarn is considered constant and independent of the tensile deformation. The loop length l is calculated according to the Kawabata model[24] as

$$l = w + 2\frac{c}{\sin\theta} + 2\pi r \tag{10}$$

where w and c are the width and length of a unit cell, respectively, r is the radius of the yarn and θ is the angle between the leg yarn and the course direction.

As illustrated in Figure 4, when a fabric is subjected to biaxial tension, the parameters $F_{c\text{fabric}}$, $F_{w\text{fabric}}$, L_w, L_c and l are known, where $F_{w\text{fabric}}$ and $F_{c\text{fabric}}(N)$ are the fabric tension parallel to the wales and courses, respectively, $L_w(mm)$ and $L_c(mm)$ are the width and length of the fabric, respectively and $l(mm)$ is the loop length.

From the Peirce model,[25] under no strain, the length of the support needle and sinker loops can be approximated as $La_0 = \frac{\pi w}{4}$. The leg length under no strain can be calculated as $Lb_0 = \frac{l-2La_0}{2} = \frac{2l-\pi w}{4}$. When the unit loops are under a tensile strain ε_w in the course direction, the needle loop, sinker loop length $La = La_0(1+\varepsilon_w)$; it is associated with the resistance RLa and the leg length Lb and its corresponding resistance RLb can be obtained by

$$La = \frac{\pi w(1+\varepsilon_w)}{4},\ Lb = \frac{2l - \pi w(1+\varepsilon_w)}{4} \tag{11}$$

$$RLa = \rho_l La = \frac{\rho_l \pi w(1+\varepsilon_w)}{4},$$

$$RLb = \rho_l Lb = \frac{\rho_l[2l - \pi w(1+\varepsilon_w)]}{4}$$

Here, ρ_l is the resistance of the yarn per unit length.

The influences of the yarn segment transfer of the loop and the contact resistance to the knitted fabric resistance are very complicated. To analyze the effect, the yarn segment transfer of the loop and the contact resistance is analyzed respectively. Figure 5 illustrates the effect of the yarn segment transfer of the loop on the fabric resistance without considering the contact resistance R_c based on the unit loop circuit model.

M x N unit loop. With the knitted loop geometry and the corresponding resistance defined, we can proceed to analyze the resistance of the entire knitted fabric circuit network with various courses and wales. We start from two courses by one wale to the general structure of m courses by n wales. In this analysis, the Kirchhoff voltage law and the loop current method are employed to calculate the total current I_1 of the fabric circuit. The Kirchhoff voltage law states that the total voltage around a closed loop must be zero. The loop current method is referred to as the mesh loop method. The independent current variables are taken to be the circulating current in each of the interior loops. First, we label the interior loop currents on a circuit diagram. Then we obtain the expressions for the change in voltage around each interior loop before solving the system of algebraic equations. Figure 6 shows the circuit diagram for a 2×1 unit loop.

If a voltage V is applied between two electrodes formed on an elastic conductive fabric, the follow equation set can be obtained from the Kirchhoff voltage law and the loop current method

$$\begin{cases} I_1\left(\frac{1}{2}RLa+\frac{1}{2}RLa+RLa+2RLb\right) \\ -I_2\left(\frac{1}{2}RLa+RLb\right)-I_3\left(\frac{1}{2}RLa+RLb\right)-I_4RLa=V \\ I_2\left(\frac{1}{2}RLa+RLb+\frac{1}{2}RLa\right)-I_1\left(\frac{1}{2}RLa+RLb\right)=0 \\ I_3\left(\frac{1}{2}RLa+RLb+\frac{1}{2}RLa\right)-I_1\left(\frac{1}{2}RLa+RLb\right)=0 \\ I_4(RLa+RLa+RLb+RLb)-I_1RLa=0 \end{cases} \tag{12}$$

A matrix equation group is used to solve the simultaneous linear equations

$$\begin{bmatrix} 2(RLa+RLb) & -(0.5RLa+RLb) & -(0.5RLa+RLb) & -RLa \\ -(0.5RLa+RLb) & RLa+RLb & 0 & 0 \\ -(0.5RLa+RLb) & 0 & RLa+RLb & 0 \\ -RLa & 0 & 0 & 2(RLa+RLb) \end{bmatrix} \begin{bmatrix} I_1 \\ I_2 \\ I_3 \\ I_4 \end{bmatrix} = \begin{bmatrix} V \\ 0 \\ 0 \\ 0 \end{bmatrix} \tag{13}$$

The total current I_1 can be obtained by Matlab software. The equivalent resistance is defined as the ratio of the voltage V and the total current I_1

$$R_{equivalent} = \frac{V}{I_1} \tag{14}$$

The total current $I_1(2,1)$ and the equivalent resistance $R_e(2,1)$ can be expressed by

$$I_1(2,1) = \frac{V(RLa+RLb)}{RLa(RLa+2RLb)} \tag{15}$$

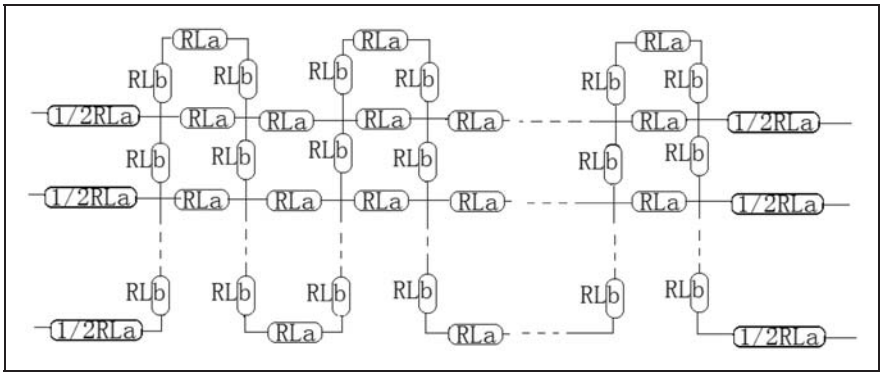

Figure 5. Fabric resistance without considering R_c.

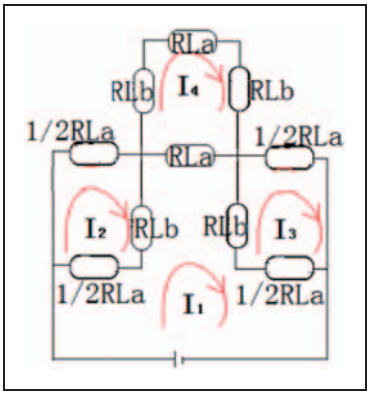

Figure 6. Resistance of 2 × 1unit loops knitted fabric.

and

$$R_e(2,1) = \frac{V}{I_1(2,1)} = \frac{RLa(RLa + 2RLb)}{RLa + RLb} \tag{16}$$

The same method is applied to $2 \times n$, $3 \times n$ and $4 \times n$ unit loop circuits. The following resistance equations of various kinds of unit loops (Table 1) can be obtained.

From Table 1, it can be obtained that

$$\begin{cases} R_{e(2,1)} = \frac{1}{2} R_{e(2,2)} = \frac{1}{3} R_{e(2,3)} \cdots = \frac{1}{n} R_{e(2,n)} \\ R_{e(3,1)} = \frac{1}{2} R_{e(3,2)} = \frac{1}{3} R_{e(3,3)} \cdots = \frac{1}{n} R_{e(3,n)} \\ R_{e(4,1)} = \frac{1}{2} R_{e(4,2)} = \frac{1}{3} R_{e(4,3)} \cdots = \frac{1}{n} R_{e(4,n)} \end{cases} \tag{17}$$

Table 1. Resistances of various kinds of unit loops.

Wale / Course	1	2	3	..	*n*
1	$2(RLa + RLb)$	$4(RLa + RLb)$	$6(RLa + RLb)$	..	$2n(RLa + RLb)$
2	$\frac{RLa(RLa+2RLb)}{RLa+RLb}$	$\frac{2RLa(RLa+2RLb}{RLa+RLb}$	$\frac{3RLa(RLa+2RLb)}{RLa+RLb}$	..	$\frac{3RLa(RLa+2RLb)}{RLa+RLb}$
3	$\frac{2RLa(RLa+RLb)(RLa+4RLb)}{3RLa^2+12RLa\times RLb+8b^2}$	$\frac{4RLa(RLa+RLb)(RLa+4RLb)}{3RLa^2+12RLa\times RLb+8b^2}$	$\frac{6RLa(RLa+RLb)(RLa+4RLb)}{3RLa^2+12RLa\times RLb+8b^2}$	..	$\frac{2nRLa(RLa+RLb)(RLa+4RLb)}{3RLa^2+12RLa\times RLb+8b^2}$
4	$\frac{RLa(RLa^2+8RLa\times RLb+8RLb^2)}{2(RLa+6RLb)(RLa+RLb)}$	$\frac{RLa(RLa^2+8RLa\times RLb+8RLb^2)}{(RLa+6RLb)(RLa+RLb)}$	$\frac{3RLa(RLa^2+8RLa\times RLb+8RLb^2)}{2(RLa+6RLb)(RLa+RLb)}$	..	$\frac{nRLa(RLa^2+8RLa\times RLb+8RLb^2)}{2(RLa+6RLb)(RLa+RLb)}$

It can be inferred that the circuit network is a multiple circuit parallel to the wale direction whereas it is in series along the course direction. Also based on the summarization and conclusion of Table 1, an m course by one wale unit loop is only needed to simplify the calculation, as shown in

$$R_{e(m,n)} = nR_{e(m,1)} \tag{18}$$

From the analysis of 2×1, 3×1 and 4×1 unit loop currents, the 2×1 unit loop current has four interior loop currents; the 3×1 unit loop current has seven interior loop currents; the 4×1 unit loop current has ten interior loop currents. It can be seen that the $m \times 1$ unit loop has $3(m-1)+1$ interior loop currents as shown in Figure 7. The total current $I_1(m,1)$ and the equivalent resistance $R_e(m,1)$ can be obtained from

$$\begin{cases}
I_1\left(\frac{1}{2}RLa+\frac{1}{2}RLa+RLa+2RLb\right) \\
\quad -I_2\left(\frac{1}{2}RLa+RLb\right)-I_3\left(\frac{1}{2}RLa+RLb\right)-I_5RLa=U \\
I_2\left(\frac{1}{2}RLa+RLb+\frac{1}{2}RLa\right)-I_1\left(\frac{1}{2}RLa+RLb\right) \\
\quad -I_4\left(\frac{1}{2}RLa\right)=0 \\
I_3\left(\frac{1}{2}RLa+RLb+\frac{1}{2}RLa\right)-I_1\left(\frac{1}{2}RLa+RLb\right) \\
\quad -I_6\left(\frac{1}{2}RLa\right)=0 \\
I_4\left(\frac{1}{2}RLa+RLb+\frac{1}{2}RLa\right)-I_2\left(\frac{1}{2}RLa\right) \\
\quad -I_5(RLb)-I_7\left(\frac{1}{2}RLa\right)=0 \\
I_5(RLa+RLa+RLb+RLb)-I_1RLa-I_4RLb \\
\quad -I_6RLb-I_8RLa=0 \\
I_6\left(\frac{1}{2}RLa+RLb+\frac{1}{2}RLa\right)-I_3\left(\frac{1}{2}RLa\right)-I_5(RLb) \\
\quad -I_9\left(\frac{1}{2}RLa\right)=0 \\
\vdots \\
\vdots \\
I_{3(m-1)-2}\left(\frac{1}{2}RLa+RLb+\frac{1}{2}RLa\right)-I_{3(m-2)-2}\left(\frac{1}{2}RLa\right) \\
\quad -I_{3(m-1)-1}(RLb)=0 \\
I_{3(m-1)-1}(RLa+RLa+RLb+RLb)-I_{3(m-2)-1}RLa \\
\quad -I_{3(m-1)-2}RLb-I_{3(m-1)}RLb-I_{3(m-1)+1}RLa=0 \\
I_{3(m-1)}\left(\frac{1}{2}RLa+RLb+\frac{1}{2}RLa\right)-I_{3(m-2)}\left(\frac{1}{2}RLa\right) \\
\quad -I_{3(m-1)-1}(RLb)=0 \\
I_{3(m-1)+1}(RLa+RLa+RLb+RLb)-I_{3(m-1)-1}RLa=0
\end{cases}$$

and

$$\begin{bmatrix}
2(RLa+RLb) & -(0.5RLa+RLb) & -(0.5RLa+RLb) & 0 & \cdots & \cdots & 0 \\
-(0.5RLa+RLb) & (RLa+RLb) & 0 & 0 & \cdots & \cdots & 0 \\
-(0.5RLa+RLb) & 0 & (RLa+RLb) & 0 & \cdots & \cdots & 0 \\
0 & -0.5RLa & 0 & (RLa+RLb) & \cdots & \cdots & 0 \\
-RLa & 0 & 0 & -RLb & \cdots & \cdots & 0 \\
0 & 0 & -0.5RLa & 0 & \cdots & \cdots & 0 \\
0 & 0 & 0 & -0.5RLa & \cdots & \cdots & 0 \\
\vdots & \vdots & \vdots & \vdots & \vdots & \vdots & \vdots \\
0 & 0 & 0 & 0 & \cdots & \cdots & 0 \\
0 & 0 & 0 & 0 & \cdots & \cdots & 0 \\
0 & 0 & 0 & 0 & \cdots & \cdots & 0 \\
0 & 0 & 0 & 0 & \cdots & \cdots & 0 \\
0 & 0 & 0 & 0 & \cdots & \cdots & 0 \\
0 & 0 & 0 & 0 & \cdots & \cdots & 0 \\
0 & 0 & 0 & 0 & \cdots & \cdots & 0 \\
\vdots & \vdots & \vdots & \vdots & \vdots & \vdots & \vdots \\
0 & 0 & 0 & 0 & \cdots & \cdots & 0 \\
0 & 0 & 0 & 0 & \cdots & \cdots & 0 \\
0 & 0 & 0 & 0 & \cdots & \cdots & 0 \\
0 & 0 & 0 & 0 & \cdots & \cdots & 0 \\
0 & 0 & 0 & 0 & \cdots & \cdots & 0 \\
0 & 0 & 0 & 0 & \cdots & \cdots & 0 \\
0 & 0 & 0 & 0 & \cdots & \cdots & 0
\end{bmatrix}
\begin{bmatrix}
I_1 \\ I_2 \\ I_3 \\ I_4 \\ I_5 \\ I_6 \\ \vdots \\ I_{3(m-1)-2} \\ I_{3(m-1)-1} \\ I_{3(m-1)} \\ I_{3(m-1)+1}
\end{bmatrix}
=
\begin{bmatrix}
U \\ 0 \\ 0 \\ 0 \\ 0 \\ 0 \\ \vdots \\ 0 \\ 0 \\ 0 \\ 0
\end{bmatrix} \tag{19}$$

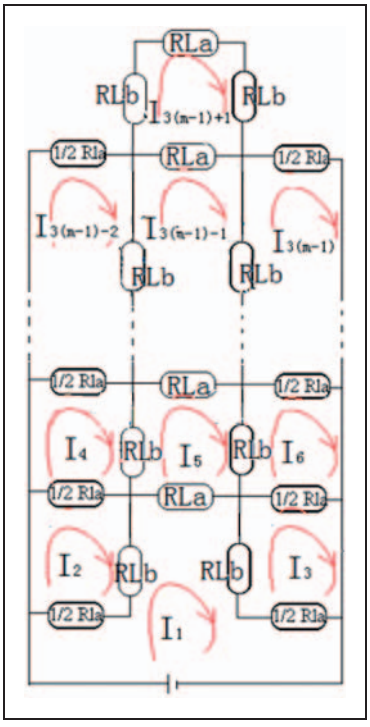

Figure 7. Resistance of $m \times 1$ unit loops knitted fabric.

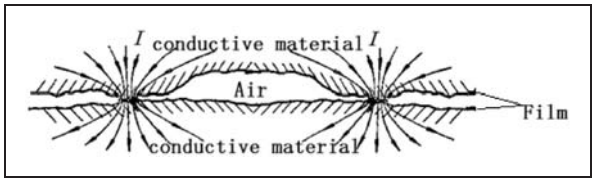

Figure 8. A schematic showing the actual contact spots and the current flow through the contacting surfaces.

Contact resistance versus strain

Contact resistance versus contact force. The contact resistance between the interlooped yarns depends on several factors including the thermophysical and mechanical properties of the materials, the characteristics of the contacting surfaces, the interstitial medium, the contact pressure, the junction temperature and the conditions surrounding the junction, as noted by Fletcher.[34]

When two conductive materials are held together, only a small fraction of the nominal surface area comes into close contact as illustrated in Figure 8. This limited actual contact area, which determines the contact resistance, is far smaller than the apparent surface because of the roughness of the contacting surfaces. When a current is imposed across the junction, the uniform current flow is contracted through the actual contact spots. Therefore, the measured contact resistance is very sensitive to the conductance of the contacting materials. Clean metallic surfaces give rise to low contact resistance while the presence of oxide films and corrosion products on the contact surfaces increase the contact resistance.

The contact resistance R_c is a series combination of constriction resistance R_s, due to the current constriction, and tunneling resistance R_f, due to the tunneling the charges through the nonconductive film located between the contacting spots as follow

$$R_c = R_{s1} + R_{s2} + R_f \tag{20}$$

In order to build an analytical model for the resistance, assumptions are considered as follows:

1. The shape of each contact area is simplified to a circle with radius a;
2. The average distance between the conductive spots is so large that the interaction between the fields of any two neighboring spots can be ignored;
3. The material is distributed homogeneously and isotropically, so that the resistivity of the material is equal everywhere and all current fields in the contact region are completely symmetrical.
4. Based on the contact theory of Holm,[22] the constriction resistance of two contacting metals can be written as

$$R_{s1} + R_{s2} = \frac{\rho_1 + \rho_2}{4a} \tag{21}$$

where a is the radius of a circle and ρ_1 and ρ_2 are the electrical resistivities of the two metals.

If these metals are the same ($\rho_1 = \rho_2 = \rho$), the constriction resistance will be

$$2R_s = \frac{\rho}{2a} \tag{22}$$

At the microscopic level, the surfaces of the two contacting materials are quite rough and the actual contact interface is the sum of the surfaces of the contacting peaks. Since the electric current flows through the small peaks, the value of the total constriction resistance is the parallel resistance of all the contact area.

Suppose n is the number of contact areas, the constriction resistance is

$$2R_{stotal} = \frac{\rho}{2na_p} \tag{23}$$

where a_p is the mean radius of the contact areas.

When the two contacting surfaces are in the atmosphere, an oxide film will form on the surface. If the oxide layer is thin enough, under a potential difference,

the electric charges can tunnel through the film. For a given external pressure and other external factors, the tunneling resistance of the film is constant.

From semiconductor theory,[35] the tunneling resistance of the film is

$$R_f = \frac{\sigma}{\pi a^2} \tag{24}$$

where σ is the thickness of the film and a is the radius of the contact area.

For n contact points on the surface with the mean radius of a_p, the total tunneling resistance of the film is

$$R_{ftotal} = \frac{\sigma}{\pi n a_p^2} \tag{25}$$

Substituting from equations (23) and (25) in equation (20), the contact resistance is

$$R_c = \frac{\rho}{2na_p} + \frac{\sigma}{\pi n a_p^2} \tag{26}$$

In general, the contact force may depend on the external parameters. And because n and a_p are determined differently, under certain material and surface conditions, the contact force is a function of n and a_p. To simplify the computational process, the relationship between the contact resistance and the contact force for two contacting materials can be written as follow

$$R_c = f(P) \tag{27}$$

where P is the contact force on the contacting materials function of f and can be determined experimentally.

Plastic deformation is initiated when a load is applied on a contacting surface. The relationship between the indentation area A and the contact force P is

$$P = HA = H\pi a^2 \tag{28}$$

where H is the contact hardness and a is the radius of the contact area.

However, this is an extremely simplified situation. In fact, in general an electrical contact area is not a smooth rigid ball in contact with a plane with a similar hardness. Moreover, for contacting surfaces with certain roughnesses and material properties, deformations are not just plastic. There are also a number of elastic deformations that occur in the contacting points. By considering these factors affecting the contacts, a correction factor ξ can be used to modify equation (28) as follow

$$P = \xi H\pi a^2 \tag{29}$$

where usually $0.2 \xi 1$. For a smooth contacting surface and plastic deformation, ξ is closer to 1.

By assuming $na_p = a$ and substituting a_p from equation (29) into equation (26), the relation between contact resistance, contact hardness, resistivity, film thickness and contact force is

$$R_c = \frac{\rho}{2}\sqrt{\frac{\pi\xi H}{P}} + \frac{\xi H\sigma}{P} \tag{30}$$

As seen in this equation, the contact resistance R_c is a function of the electrical resistivity of the material ρ, the contact hardness H, the thickness of the film σ and the contact force P. In general, this equation is still complex to calculate, so the empirical formula is used to simplify the calculation process.

According to Holm's theory, the contact resistance of a conductor is inversely proportional to the contact area, the change in surface area depends on the normal force and the electrical contact is ideally a smooth rigid ball in contact with a plane. Based on this model the relationship between contact radius and contact force is

$$a \propto P^m \tag{31}$$

where $m = 1/3$ for elastic deformation and $m = 1/2$ for plastic deformation.

By assuming $na_p = a$ and substituting a from equation (30) into equation (31), the relationship between the contact resistance and the normal force at interlooped yarns can be empirically described by a power equation

$$R_c = KF_t^{-\mathrm{m}} \tag{32}$$

where based on the experimental result, two contacting materials are considered to be in point–point contact (ball–ball, ball–plane and columnar–columnar) with $m = 0.5$, two contact materials are considered to be in line–line contact (columnar–plane) with $m = 1$ and K depends on the resistivity ρ and hardness H of the contacting materials.

Contact force in a knitted fabric. Since the loop yarn segment is repeated along the wale and course directions, we proceed to examine the contact resistance at yarn interlooping points of a knitted stitch. During the elongation and recovery of the knitted fabric deformation process, the contact resistance on interlooping yarns changes with its corresponding contact force. As illustrated in Figure 9, the interlooped yarns in a knitted fabric have several contact areas which result in an internal friction force between the contacting yarns. The relationship between the normal force on

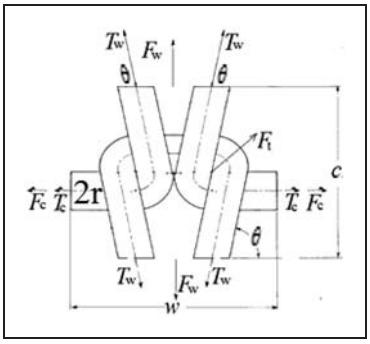

Figure 9. A basic element of the structure.

interlooping yarns and the contact resistance can be obtained experimentally.

To obtain a relationship between the contact resistance and the contact force we assume the following:

1. The resistance of a unit length of the yarn is constant and independent of the tensile deformation;
2. The contact resistance of two interlooped yarns only depends on the normal contact force at the crossover regions regardless of their contact length.

When the fabric is subjected to biaxial tension, the following parameters $F_{wfabric}$, $F_{cfabric}$, L_w, L_c and l are presumably known. Figure 9 shows the biaxial tension to the basic mechanical element of the structure.

T_w is the tension along the wale stretch, T_c is the tension along the course stretch, F_t is the normal force at the interlooped yarns and r and θ are the same parameters as those defined and used in Figure 4(b).

From the definition of the fabric stress

$$\begin{cases} S_w = \dfrac{F_w}{w} = \dfrac{F_{w\text{fabric}}}{L_w} \\ S_c = \dfrac{F_c}{c} = \dfrac{F_{c\text{fabric}}}{L_c} \end{cases} \tag{33}$$

where $F_{c\text{fabric}}$, $F_{w\text{fabric}}$, L_w, L_c, w and c are the same parameters as those defined and used in Figure 4, S_w is the fabric stress along the wale stretch (vertical stress), S_c is the fabric stress along the course stretch (horizontal stress), F_w is the fabric tension in a unit structure along the wale stretch (vertical tension) and F_c is the fabric tension in a unit structure along the course stretch (horizontal tension).

From Figure 9, it can be seen that

$$\begin{cases} F_w = 2T_w \sin\theta \\ F_c = T_c \end{cases} \tag{34}$$

Substituting F_w and F_c from equation (33) into equation (34),

$$\begin{cases} T_w = \dfrac{S_w w}{2\sin\theta} \\ T_c = S_c c \end{cases} \tag{35}$$

and

$$\frac{T_w}{T_c} = \frac{wS_w}{2cS_c\sin\theta} \tag{36}$$

The yarn inclination can be expressed as

$$\tan\theta = \frac{c}{2r} \tag{37}$$

So

$$\sin\theta = \frac{1}{\sqrt{1+(\frac{2r}{c})^2}} \tag{38}$$

From the definition of fabric parameters

$$\begin{cases} w = \frac{L_w}{n} \\ c = \frac{L_c}{m} \end{cases} \tag{39}$$

By substituting from equations (35) and (38) into equation (39)

$$\begin{cases} T_w = \frac{S_w L_w \sqrt{1+(\frac{2mr}{L_c})^2}}{2n} \\ T_c = \frac{S_c L_c}{m} \end{cases} \tag{40}$$

From the Kawabata model,[24] the contacting force can be seen as

$$F_t = \begin{cases} \sqrt{T_w^2 + T_c^2}\cos\left[\dfrac{\pi}{4} - \tan^{-1}\left(\dfrac{T_w}{T_c}\right)\right] \ldots \text{ for } \varepsilon_w > \varepsilon_c \\ \sqrt{T_w^2 + T_c^2} \ldots \text{ for } \varepsilon_w = \varepsilon_c \\ \sqrt{T_w^2 + T_c^2}\cos\left[\dfrac{\pi}{4} - \tan^{-1}\left(\dfrac{T_c}{T_w}\right)\right] \ldots \text{ for } \varepsilon_w < \varepsilon_c \end{cases} \tag{41}$$

where ε_w is the tensile strain along the course stretch and ε_c is the tensile strain along the wale stretch.

By substituting T_w and T_c from equation (40) into equation (41), it can be seen that F_t is a function of S_w,

S_c, L_w, L_c, m, n and r for three different regimes as follow.

$$F_t = \begin{cases} \sqrt{\left(\frac{S_w L_w \sqrt{1+(\frac{2mr}{L_c})^2}}{2n}\right)^2 + \left(\frac{S_c L_c}{m}\right)^2} \cos\left[\frac{\pi}{4} - \tan^{-1}\left(\frac{mS_w L_w \sqrt{1+(\frac{2mr}{L_c})^2}}{2nS_c L_c}\right)\right] \ldots \text{ for } \varepsilon_w > \varepsilon_c \\ \sqrt{\left(\frac{S_w L_w \sqrt{1+(\frac{2mr}{L_c})^2}}{2n}\right)^2 + \left(\frac{S_c L_c}{m}\right)^2} \ldots \text{ for } \varepsilon_w = \varepsilon_c \\ \sqrt{\left(\frac{S_w L_w \sqrt{1+(\frac{2mr}{L_c})^2}}{2n}\right)^2 + \left(\frac{S_c L_c}{m}\right)^2} \cos\left[\frac{\pi}{4} - \tan^{-1}\left(\frac{2nS_c L_c}{mS_w L_w \sqrt{1+\left(\frac{2mr}{L_c}\right)^2}}\right)\right] \ldots \text{ for } \varepsilon_w < \varepsilon_c \end{cases} \quad (42)$$

Conclusion

Based on the hexagon resistance model and the mechanical properties, the effect of the yarn segment transfer of the loop on knitted fabric resistance is analyzed. A circuit model based on the theory with textile mechanisms is proposed to simulate the sensing mechanism and validate the reliability of the sensor. Holm's electrical contact theory and the classical knitted fabric mechanics model of Kawabata[24] and Popper[30] are used to calculate the relationship between the contact resistance and the contact force in an elastic fabric sensor. It was found that the circuit network is a multiple circuit parallel to the wale direction whereas it is in series along the course direction; the contact resistance of the overlapped yarns in the fabric decreases as a power-law function with the contact force. This theoretical study can instruct the design of wearable sensors.

Funding

We would like to extend thanks to the colleagues at the Advanced Fiber Materials Laboratory (AFML) and at the Flexible Electronics and Energy Lab (FEEL) at the University of British Columbia for their help and support. We would like to thank the Canada Foundation for Innovation and the Multidisciplinary University Research Initiative for supporting this research. We would like to thank Donghua University for supporting this research through a project titled Fundamental Research Funds for the Central Universities, and we would like to thank the State Scholarship Fund for supporting this research through a project titled the China Scholarship Council (CSC) Fund for a PhD student (No. 2011663022).

References

1. Gulley SP, Rasch EK and Chan L. If we build it, who will come? Working-age adults with chronic health care needs and the medical home. *Medical Care* 2011; 49: 149–155.
2. Gulley SP, Rasch EK and Chan L. Ongoing coverage for ongoing care: access utilization, and out-of-pocket spending among uninsured working-aged adults with chronic health care needs. *Am J Public Health* 2011; 101: 368–375.
3. Hazinksi MF and Markenson D. Response to cardiac arrest and selected life-threatening medical emergencies: the medical emergency response plan for schools: a statement for healthcare providers, policymakers, school administrators, and community leaders. *Circulation* 2004; 109: 278–291.
4. Teng XF, Zhang YT, Poon CC, et al. Wearable medical systems for p-Health. *IEEE Reviews Biomed Engr* 2008; 1: 62–74.
5. Bonato P. Wearable sensors and systems. From enabling technology to clinical applications. *IEEE Eng Med Biol Mag* 2010; 29: 25–36.
6. Karantonis DM, Narayanan MR and Mathie M. Implementation of a real-time human movement classifier using a triaxial accelerometer for ambulatory monitoring. *IEEE Trans Info Tech Biomed* 2006; 10: 156–167.
7. Parkka J, Ermes M and Korpipaa P. Activity classification using realistic data from wearable sensors. *IEEE Trans Info Tech Biomed* 2006; 10: 119–128.
8. Ní Scanaill C, Carew S and Barralon P. A review of approaches to mobility telemonitoring of the elderly in their living environment. *Ann Biomed Engr* 2006; 34: 547–563.
9. Luprano J, Sola J, Dasen S, et al. Combination of body sensor networks and on-body signal processing algorithms: the practical case of MyHeart project. In *Proc. of International Workshop on Wearable and Implantable Body Sensor Networks: 76–79*, MIT, Cambridge, USA, April, 2006.

10. Anlike U, Ward JA, Lukowicz P, et al. AMON: a wearable multiparameter medical monitoring and alert system. *IEEE Trans Info Tech Biomed* 2004; 8(4): 415–427.
11. Linz T, Kallmayer C, Aschenbrenner R et al. Fully integrated EKG shirt based on embroidered electrical interconnections with conductive yarn and miniaturized flexible electronics. In: *International workshop on wearable and implantable body sensor networks*, Cambridge, USA, 3–5 April, 2006, pp. 23-26.
12. Noury N, Dittmar A, Corroy C et al. A smart cloth for ambulatory telemonitoring of physiological parameters and activity: the VTAMN project. In: *International workshop on enterprise networking and computing in healthcare industry*, 2004, vol. 6(28), pp. 155–160.
13. Poon CC and Zhang YT. Cuff-less and noninvasive measurements of arterial blood pressure by pulse transit time. In: *27th annual international conference of the IEEE engineering in medicine and biology society*, Shanghai, China, 2005, pp. 5877–5880.
14. Teng XF and Zhang YT. The effect of contacting force photoplethysmographic signals. *Physiolog Measure* 2004; 25(5): 1323–1335.
15. Yan YS, Poon CC and Zhang YT. Reduction of motion artifact in pulse oximetry by smoothed pseudo Wigner-Ville distribution. *Neuroengr Rehab* 2005; 2(3): 1–9.
16. Bao SD, Zhang YT and Shen LF. A design proposal of security architecture for medical body sensor networks. In: *International workshop on wearable and implantable body sensor networks*, Cambridge, USA, 3–5 April 2006, pp. 84–90.
17. Zhang YT, Poon CC, Chan CH et al. CURS: a health-shirt using e-textile materials for the continuous and cuff-less monitoring of arterial blood pressure. In: *3rd IEEE-EMBS international summer school and symposium on medical devices and biosensors*, Cambridge, USA, 2006, pp. 86–89.
18. Xiang XY, Poon CC and Zhang YT. Modeling of the cuff-less blood-pressure measurement errors for the evaluation of a wearable medical device. In: *3rd IEEE-EMBS international summer school and symposium on medical devices and biosensors*, Cambridge, USA, 2006, pp. 105–108.
19. Rossi DD, Santa AD and Mazzoldi A. Dressware: wearable hardware. *Mat Sci Engine C* 1999; 7: 31–35.
20. Wu WL, Hamada H and Meakawa Z. Computer simulation of the deformation of weft knitted fabrics for composite materials. *Text Inst* 1994; 85: 198–214.
21. Araujo MD, Fangueiro R and Hong H. Modelling and simulation of the mechanical behaviour of weft-knitted fabrics for technical applications, part III: 2D hexagonal FEA model with non-linear truss elements. *Autex Res* 2004; 4(1): 25–32.
22. Holm R. *Electric contacts*, 4th ed. Berlin/New York: Springer-Verlag, 1967, pp.7–19.
23. William MM and William RM. *The bonded electrical resistance strain gage: An introduction*. Oxford, UK: Oxford University Press, 1992.
24. Kawabata S. Nonlinear mechanics of woven and knitted materials. In: Chou TW and Ko FK (eds) *Textile structural composites*. Amsterdam: Elsevier, 1989.
25. Peirce FT. Geometrical principles applicable to tie design of functional fabrics. *Text Res* 1947; 17: 123–147.
26. Hepworth B and Leaf GAV. Shape of the loops in an undeformed plain weft knit fabric, studies in modern fabrics: a report on the 1970 diamond jubilee conference of the textile institute, part 2. *Text Inst Ind* 1970; 8: 209 –213.
27. Munden DL. The geometry and dimensional property of plain-knit fabrics. *Text Inst* 1959; 50: 448 – 471.
28. Postle R and Munden DL. Analysis of the dry-relaxed knitted loop configuration. *Text Inst* 1967; 58: 329 –365.
29. Shanahan WJ and Postle R. A theoretical analysis of the plain knitted structure. *Text Res* 1970; 40: 656–665.
30. Popper P. The theoretical behavior of a knitted fabric subjected to biaxial stresses. *Text Res* 1966; 36(2): 148–157.
31. Loginov A, Grishanov S and Harwood R. Modelling the load-extension behaviour of plain-knitted fabric. Part I: a unit-cell approach towards knitted-fabric mechanics. *Text Inst* 2002; 93: 218–238.
32. Loginov A, Grishanov S and Harwood R. Modelling the load-extension behaviour of plain-knitted fabric. Part III: model implementation and experimental verification. *Text Inst* 2002; 93: 251–275.
33. Loginov A, Grishanov S and Harwood R. Modelling the load-extension behaviour of plain-knitted fabric. Part 2: Energy relations in the unit cell. *Text Inst* 2002; 93: 239–250.
34. Fletcher LS. Recent developments in contact conductance heat transfer. *ASME Heat Transfer* 1988; 110: 1059–1070.
35. Wang S. *Fundamentals of semiconductor theory and device physics*. New Jersey: Prentice Hall, 1989.